energies

MDPI

Article

A Day-Ahead Economic Dispatch Method for Renewable Energy Systems Considering Flexibility Supply and Demand Balancing Capabilities

Zheng Yang [1], Wei Xiong [1], Pengyu Wang [2], Nuoqing Shen [2,*] and Siyang Liao [2]

[1] Central China Branch of State Grid Corporation of China, Wuhan 430077, China; ytz1994@hotmail.com (Z.Y.); xiongw86@126.com (W.X.)
[2] School of Electrical Engineering and Automation, Wuhan University, Wuhan 430072, China; 2023102070046@whu.edu.cn (P.W.); liaosiyang@whu.edu.cn (S.L.)
* Correspondence: 2020302192085@whu.edu.cn; Tel.: +86-188-0729-2729

Abstract: The increase in new energy grid connections has reduced the supply-side regulation capability of the power system. Traditional economic dispatch methods are insufficient for addressing the flexibility limitations in the system's balancing capabilities. Consequently, this study presents a day-ahead scheduling method for renewable energy systems that balances flexibility and economy. This approach establishes a dual-layer optimized scheduling model. The upper-layer model focuses on the economic efficiency of unit start-up and shut-down, utilizing a particle swarm algorithm to identify unit combinations that comply with minimum start-up and shut-down time constraints. In contrast, the lower-layer model addresses the dual uncertainties of generation and load. It employs the Generalized Polynomial Chaos approximation to create an opportunity-constrained model aimed at minimizing unit generation and curtailment costs while maximizing flexibility supply capability. Additionally, it calculates the probability of flexibility supply-demand insufficiency due to uncertainties in demand response resource supply and system operating costs, providing feedback to the upper-layer model. Ultimately, through iterative solutions of the upper and lower models, a day-ahead scheduling plan that effectively balances flexibility and economy is derived. The proposed method is validated using a simulation of the IEEE 30-bus system case study, demonstrating its capability to balance system flexibility and economy while effectively reducing the risk of insufficient supply-demand balance.

Keywords: renewable energy system; flexibility supply-demand balance; generalized polynomial chaos; dual-layer optimization; day-ahead dispatch

check for updates

Citation: Yang, Z.; Xiong, W.; Wang, P.; Shen, N.; Liao, S. A Day-Ahead Economic Dispatch Method for Renewable Energy Systems Considering Flexibility Supply and Demand Balancing Capabilities. *Energies* **2024**, *17*, 5427. https://doi.org/10.3390/en17215427

Academic Editors: Javier Contreras and Pierluigi Siano

Received: 28 September 2024
Revised: 22 October 2024
Accepted: 26 October 2024
Published: 30 October 2024

Copyright: © 2024 by the authors. Licensee MDPI, Basel, Switzerland. This article is an open access article distributed under the terms and conditions of the Creative Commons Attribution (CC BY) license (https://creativecommons.org/licenses/by/4.0/).

1. Introduction

Under the strategic framework of the dual-carbon target, the installed capacity of new energy in China has shown rapid growth. However, new energy generation methods including wind power and photovoltaic power generation have inherent uncertainty. Apart from that, the high proportion of new energy connected to the grid has led to a significant decline in the power-side regulation capability of the power system [1], and the traditional source-follows-load balance model has been broken, making the security stability and economy of the power system challenged, and bringing to the fore the issue of grid supply-demand balance.

The flexibility of new power systems is characterized by directional features, multi-temporal and spatial aspects, state dependence, and probabilistic characteristics [2]. To accurately describe the uncertainty in power systems, it is necessary to construct appropriate probabilistic statistical models. This framework allows for the evaluation and analysis of system flexibility. Thus, a unified mathematical framework is required to assess probabilistic flexibility across various temporal and spatial scales and different scenarios.

Addressing the issue of insufficient system flexibility due to the increasing proportion of renewable energy, ref. [3] emphasizes the importance of accurately characterizing random disturbance events while fully exploring flexibility resources from generation, grid, load, and storage. Study [4] quantifies the benefits of coordinated planning among generation, grid, and storage in high-renewable power systems through sensitivity analysis. Ref. [5] proposes a resource allocation method that accounts for the uncertainty of renewable energy, enhancing the system's flexible adjustment capacity. Ref. [6] establishes a continuous proactive optimization model to jointly optimize energy and flexible services.

In the context of day-ahead scheduling for new power systems, ref. [7] introduces a resident flexible load optimization scheduling method that considers random resident behavior. In [8], a chance-constrained stochastic programming model is constructed that balances economic and reliability concerns. Study [9] incorporates network topology optimization techniques into the scheduling framework to examine their synergistic effects. Ref. [10] proposes an optimization scheme for a gas-electric integrated energy system with bidirectional energy flow. In [11], a robust dual model is developed for a virtual power plant that includes electric vehicles, although it does not address renewable energy consumption issues. Ref. [12] presents a low-carbon economic scheduling model for high-renewable energy consumption. Additionally, ref. [13] optimizes electric vehicle parameters using least squares estimation, while in [14], a distribution network planning model is established that considers the flexibility of electric vehicle virtual power plants and high photovoltaic penetration. Research study [15] proposes a scheduling strategy that accounts for both wind and solar energy absorption as well as the flexibility of electric vehicles. Ref. [16] addresses the uncertainty of renewable energy output by developing a forecasting model and proposing a multi-objective optimization scheduling method.

In [17], a day-ahead scheduling strategy is presented for integrated energy systems that balances supply and demand-side flexibility. Ref. [18] constructs a two-stage distributed economic scheduling model to address uncertainties related to large-scale distributed energy integration. Research study [19] proposes a revised scheduling model for new power systems aimed at resolving insufficient supply and demand flexibility. Ref. [20] introduces an optimization scheduling method for coal-water-wind-solar multi-energy systems to mitigate the negative impacts of renewable energy. In [21], a coordinated scheduling strategy is proposed for independent microgrids but does not consider resource uncertainty. Research study [22] comprehensively evaluates the flexibility and uncertainty factors of multi-energy systems. Ref. [23] develops a hierarchical coordinated optimization scheduling model for multi-energy power systems that balances flexibility, complementarity, stability, economy, and cleanliness. Ref. [24] fully accounts for the comprehensive flexibility of generation, load, and storage in the optimization scheduling process. Although existing research largely explores flexibility from the perspective of supply-demand balance, there remains a lack of probabilistic statistical evaluation models and insufficient consideration of the grid's power transmission capacity.

This research addresses the challenges associated with the integration of renewable energy sources by defining a flexible supply and demand balance index and constructing an opportunity constraint model. This framework facilitates the measurement of system flexibility in relation to supply, demand, and power transmission. A two-layer optimized scheduling model is proposed, which considers both the economic and flexible operation of the system. The study employs the Generalized Polynomial Chaos (gPC) approximation principle to effectively characterize tidal trend uncertainty influenced by multiple factors. This approach incorporates the flexible supply capacity of demand response resources, enhancing the system's adjustable potential and its ability to balance uncertainties in bilateral active power from generation and load.

The paper is organized as follows: Section 2 defines system flexibility and its quantitative indicators. Section 3 details the gPC method, including orthogonal polynomials and their application in this context. Section 4 presents the two-layer scheduling model, outlining the modeling ideas and optimization process. Section 5 includes a calculated

simulation to evaluate the proposed scheduling strategies, followed by a summary in Section 6 that highlights the main findings and implications of the study.

2. Definition of System Flexibility and Quantitative Indicators

Power system flexibility is manifested as power supply flexibility and grid flexibility [25], both of which affect the system's flexibility supply-demand balance. The former reflects the abundance of system flexibility supply relative to its demand, and the latter shows the transmission capacity of the grid. In this study, flexibility supply/demand balance metrics are constructed to quantify the power flexibility, accurately characterize the current uncertainty and model the opportunity constraints based on the principle of generalized polynomial chaos approximation to consider the line power transfer margin.

2.1. Flexibility Requirements

The system flexibility requirement mainly stems from the uncontrollable change of power, which is viewed as the prediction error of the wind load. Let $\varepsilon_t^{WT}, \varepsilon_t^{PV}$ and ε_t^L represent the random variables for the wind power, photovoltaic power, and load prediction error at time t, respectively. The net load prediction error ε_t^D at time t is then defined as the system flexibility requirement, as follows:

$$\varepsilon_t^D = \varepsilon_t^L - \left(\varepsilon_t^{WT} + \varepsilon_t^{PV}\right). \tag{1}$$

By the principle of probabilistic convolution operation, the random variable addition and subtraction operation can be represented by the convolution operation of the probability density function, i.e.:

$$\varphi_t^N = \int_{-\infty}^{+\infty} \varphi_t^{WT}(\tau) \cdot \varphi_t^{PV}(x-\tau)d\tau, \tag{2}$$

$$\varphi_t^D = \int_{-\infty}^{+\infty} \varphi_t^L(\tau) \cdot \varphi_t^N(-x-\tau)d\tau, \tag{3}$$

where $\varphi_t^D, \varphi_t^I, \varphi_t^{WT}$ and φ_t^{PV} refer to the probability density function of the system flexibility requirement, the prediction error of the load, wind power and photovoltaic power, respectively. φ_t^N denotes the probability density function of the prediction error of the sum of the wind power and photovoltaic power generation of the system.

2.2. Flexibility of Supply

System flexibility supply is defined as the adjustment ability of various flexible resources of the system to cope with power disturbance. $X_{i,t}$ is set into random variables of class i resource adjustable ability at time t. The system flexibility supply X_t at time t can be expressed as follows:

$$X_t = \sum_{i \in S} X_{i,t}, \tag{4}$$

where, S refers to the set of adjustable resources.

The probability density function of the system flexibility supply can be written as follows:

$$\varphi_t^S = \mathop{\oplus}_{i \in S} \varphi_{X_{it}}, \tag{5}$$

where φ_t^s and $\varphi_{X_{i,t}}$ denote the probability density function of the system flexibility supply and the adjustable capacity of resource i at moment t, respectively; and $\oplus$ denotes the convolution sum operation.

2.3. Flexible Quantitative Index of Supply and Demand Balance

The flexible supply and demand balance refers to the extent the flexible supply of various resources exceeds the allowable level relative to the flexibility demand at any time, at the time scale and in any direction.

Both the flexibility supply and demand are random variables following a specific distribution. $\gamma_t = X_t - \varepsilon_t^D$ is defined as the random variable of the system flexibility margin at time t, and $\varphi_{y_t} = \int_{-\infty}^{+\infty} \varphi_t^S(\tau) \cdot \varphi_t^D(-x-\tau)d\tau$ represents the corresponding probability density function. The supply and demand balance of the system flexibility can be described as the probability that the system flexibility margin is less than 0 or the expectation is lower than the given threshold, namely:

$$P_M = \int_{-\infty}^{0} \varphi_{\gamma_t}(x)dx \leq \theta, \tag{6}$$

$$E_M = -\int_{-\infty}^{0} x \cdot \varphi_{\gamma_t}(x)dx \leq \xi, \tag{7}$$

where P_M and E_M denote the probability and threshold, respectively, for measuring the supply-demand balance of the system flexibility; and θ and ξ denote the probability threshold and expectation threshold, respectively, for measuring the supply-demand balance of the system flexibility.

The probability distribution function φ_{γ_t} of the flexibility margin in Figure 1 corresponds to the insufficient/sufficient flexibility scenarios in the left/right half planes. The quantitative relationship between flexibility and the level of renewable energy consumption and the risk of load loss can be constructed through calculating the relevant numerical characteristics of φ_{γ_1}, as shown in Figure 1. The physical meaning of the inflexibility probability index is the ratio of the inflexibility deficit time to the total time during the study period; the inflexibility expectation index is in proportion to the amount of wind/photovoltaic power abandoned or load loss, and the value of the inflexibility deficit for a given threshold reflects the ideal value of the additional flexibility resources required to obtain a given level of flexibility in the system.

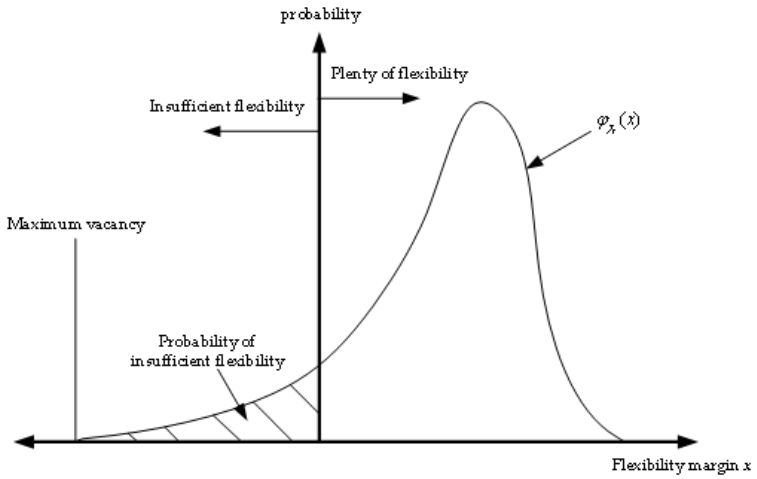


Figure 1. Physical implications of system flexibility measurement indicators.

3. Generalized Polynomial Chaos Method

The distribution characteristics of grid currents become particularly complex due to the uncertainties and varying probability distributions associated with both the wind power and system load. The Generalized Polynomial Chaos (gPC) method, an effective tool for uncertainty quantification [26], enables the accurate representation of complex random variables through polynomial approximation. Therefore, this study employs the principle of gPC approximation to characterize the tidal current uncertainty under the

combined influence of multiple uncertainty factors. This approach further mitigates the risk of network congestion and ensures the safe and stable operation of the power grid.

3.1. Orthogonal Polynomials and Their Construction Methods

If $\{Q_k(x)\}(k = 0, 1, 2, M)$ is an orthogonal polynomial system, where M is a non-negative integer, then:

$$\begin{cases} \int Q_i(x)Q_j(x)\omega(x)dx = 0, i \neq j, \\ \int Q_i(x)Q_j(x)\omega(x)dx \neq 0, i = j \end{cases} \tag{8}$$

where i and j indicate the order of the polynomials, and $\omega(x)$ denotes the orthogonal weight function.

Setting N to be a non-negative integer, if $S = \{0, 1 \cdots\}$ or $S = \{0, 1 \cdots, N\}$, when $\forall n \in S, n$-order polynomial $Q_n(x)$ is expressed as follows:

$$Q_n(x) = \sum_{i=0}^{n} a_i x^i, \tag{9}$$

If the polynomial $\{Q_n(x), n \in S\}$ satisfies Formula (10), it is called an orthogonal polynomial system.

$$\int Q_n(x)Q_m(x)\omega(x)dx = \gamma_n \delta_{nm}, \tag{10}$$

where δ_{nm} refers to the Kronecker operator, i.e., $\delta_{nm} = 0$ when $m = n, \delta_{nm} = 1, m \neq n$; γ_n is the normalization constant.

Therefore, when $m = n$, Equation (11) is expressed as follows:

$$\gamma_n = \int Q_n^2(x)\omega(x)dx. \tag{11}$$

In the Askey orthogonal polynomial lines, there are four common orthogonal polynomials, as displayed in Table 1.

Table 1. The optimal correspondence between Askey orthogonal polynomial types and continuous random variable types.

Random Variable Type	The Orthogonal Polynomial Type	Weight Function for Defining the Domain
normal distribution	Hermite	$(-\infty, +\infty)$
Gamma distribution	Lagurre	$[0, \infty)$
Beta distribution	Jacobi	[a, b]
hypodispersion	Legendre	[a, b]

Orthogonal polynomials for any weight function can be constructed via Gram–Schmidt.

3.2. Basis Function of the gPC

The basis functions in the gPC method are constructed based on the probability density functions corresponding to each mutually independent random variable. The vector of independent random variables is set to be $x = (x_1, x_2, \cdots, x_d)^T$, and the corresponding probability density functions are $\rho_{x_1}(x_1), \rho_{x_2}(x_2), \ldots, \rho_{x_d}(x_d)$. The orthogonal polynomial system corresponding to each independent random variable in x is built, denoted as $\left\{\phi_k^{x_1}(x_1)\right\}\left\{\left\{\phi_k^{x_2}(x_2)\right\}, \ldots \backslash \left\{\phi_k^{x_d}(x_d)\right\}\right.$, where $k = 0, 1, \ldots, r$, respectively, and the orthogonal polynomial basis function system in this case is obtained in the form of a tensor product:

$$\Phi_k(x) = \phi_{k_1}^{x_1}(x_1)\phi_{k_2}^{x_2}(x_2) \ldots \phi_{k_d}^{x_d}(x_d), \tag{12}$$

where $(k_1, k_2, \ldots, k_d)$ is all the non-negative integer solutions satisfying $0 \leq \sum_{i=1}^{s} k_i \leq r$, including C_{r+d}^{d} combinations; $\boldsymbol{k} = (k_1, k_2, \cdots, k_d); \sum_{i=1}^{d} k_i$ refers to the order of the basis function.

3.3. The gPC Approximation and the Probability Features

When N is set as a non-negative integer, and Z is a one-dimensional random variable, the N-order generalized polynomial chaos approximation of the function $f(Z)$ is expressed as:

$$f(Z) \approx f_N(Z) = \sum_{i=0}^{N} f_i \Phi_i(Z), \tag{13}$$

$$f_i = \frac{1}{\gamma_i} E(f(Z)\phi_i(Z)), \tag{14}$$

where f_i is the approximation coefficient of $f(Z)$ under the basis function $\Phi_i(Z)$; $\Phi_i(Z)$ is the basis function of the orthogonal polynomial of order i, and E is the expectation operator.

After obtaining the **N**-order polynomial expansion expression of $f(Z)$, various statistical properties can be derived. Specifically, the expected value of $f(Z)$ corresponds to the coefficient of its zero-order term, as follows:

$$\mu_f = E(f(Z)) \approx E\left(\sum_{i=0}^{N} f_i \Phi_i(Z)\right) = \sum_{i=0}^{N} f_i \int \Phi_i(Z)\rho(Z)dz = f_0. \tag{15}$$

The variance of $f(Z)$ is expressed as follows:

$$Var_f = E\left(\left(f(Z) - \mu_f\right)^2\right) = \sum_{i=0}^{N}\left(\gamma_i f_i^2\right). \tag{16}$$

The probability density function of $f(Z)$ can be calculated by sampling Z using the Monte Carlo method and combining with gPC expression.

4. A Two-Layer Optimized Scheduling Model Considering the Flexible Supply and Demand Balance Capability

4.1. Modeling Ideas

The two-layer optimized scheduling model for renewable energy systems, which considers the flexible balancing capability of supply and demand, is illustrated in Figure 2. The upper model determines the optimal start and stop strategy, employing a particle swarm algorithm to generate unit combinations that meet start and stop time constraints, as well as the associated costs. Based on the gPC approximation principle, the lower model constructs an opportunity constraint model that adheres to system flexibility requirements while minimizing operational costs. It optimizes unit output according to the combinations established by the upper model, ensuring that units provide adequate flexibility to address uncontrollable power fluctuations from both sources and loads. The lower model assesses whether the system's flexibility under the current unit combination meets requirements. If flexibility is insufficient, the model calculates the operational costs and adds a penalty term for inadequate flexibility, which is then fed back to the upper model. The upper model adjusts and updates the particle swarm position information, iteratively searching for the generator set that satisfies the supply and demand balance criteria for system flexibility while achieving the optimal start and stop plan. Additionally, the power flow opportunity constraint maintains a margin for the flexibility of the power grid, considering the unit start and stop costs, wind and solar curtailment costs, generation costs, and the system flexibility index comprehensively.

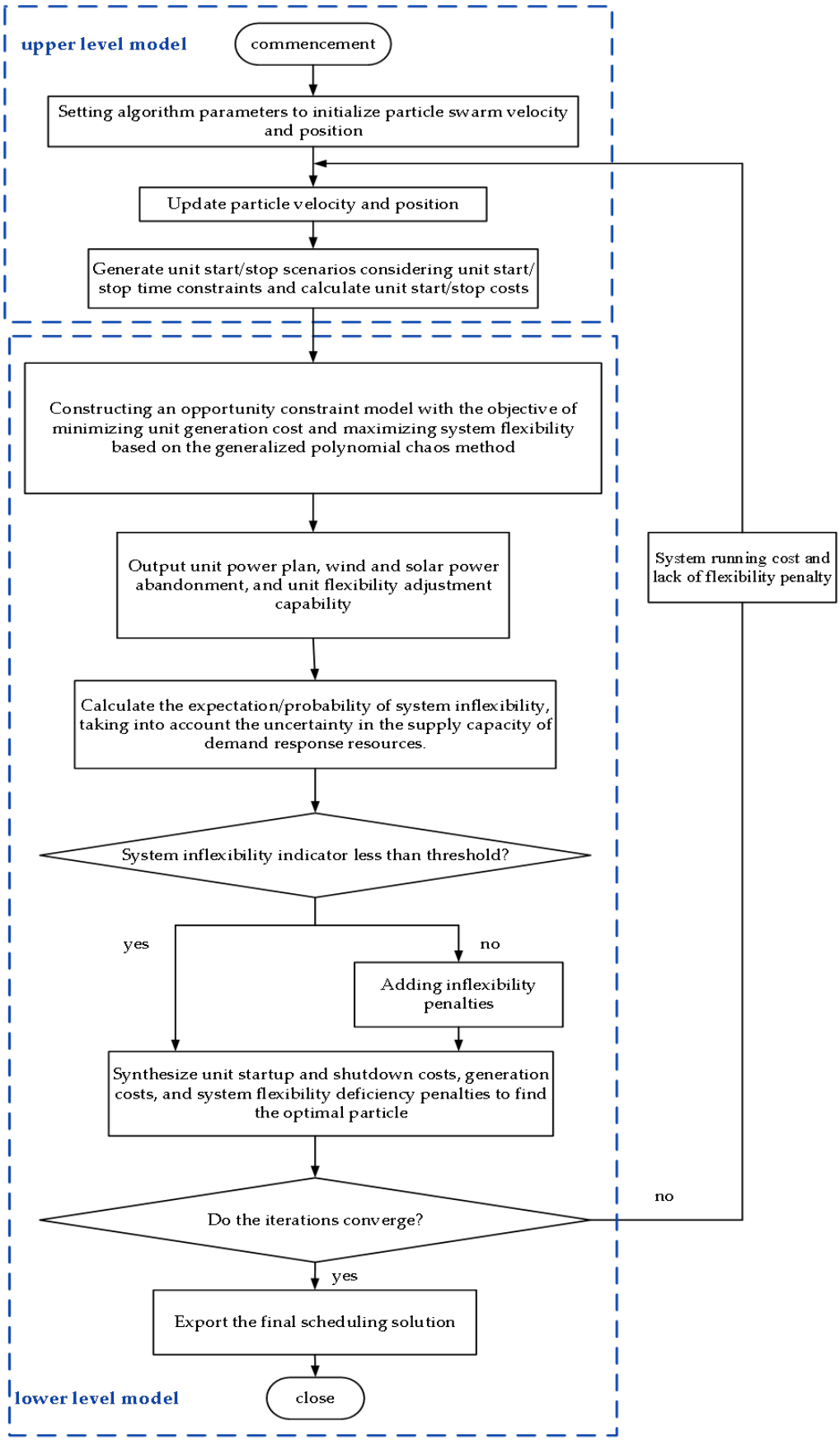


Figure 2. Flowchart of dual-layer optimization scheduling model.

The lower-level model determines the day-ahead generation schedule and the flexibility-adjustable capacity of each unit. This study takes into account the uncertain supply capacity of electric vehicle and air-conditioning clusters, establishing a probabilistic assessment model for their day-ahead adjustable capacity. This model aims to acquire the probability distribution of the adjustable capacity of demand-response resources at each moment, utilizing the assessment method from prior research [27]. The overall system's flexibility supply capacity is expressed as the combination of the deterministic unit adjustable capacity and the statistically significant demand-response adjustable capacity, effectively leveling the probability distribution. Furthermore, the probability density function of the system flexibility can be derived through the aggregation of the system flexibility supply and the flexibility demand. The flexibility deficit index of the system at each moment can be quantitatively calculated.

The optimal scheduling scheme is sought by considering the unit start-stop costs, wind and solar curtailment costs, generation costs, and measures of system flexibility, continuing until the model converges.

4.2. Model Building

4.2.1. The Upper Model

The unit combination scheme shall consider the unit start-stop time constraints, as shown in the following formula:

$$\sum_{k=t}^{t+T_{S,i}-1} (1-u_{i,k}) \geq T_{S,i}(u_{i,t-1}-u_{i,t}), \tag{17}$$

$$\sum_{k=t}^{t+T_{o,i}-1} u_{i,k} \geq T_{O,i}(u_{i,t}-u_{i,t-1}), \tag{18}$$

where $u_{i,k}$ is the binary variable, indicator +e is the state of unit i at time k; when $u_{i,k}=1$, the unit is running, while when $u_{i,k}=0$, the unit is shut down; $T_{S,i}$ signifies the minimum shutdown time and $T_{O,i}$ is the minimum start-up time.

4.2.2. The Lower Model

1. Objective function

Based on the upper unit combination scheme, the lower unit output plan is reasonably arranged to provide sufficient flexible supply capacity. According to the source and load uncertainty factor, the fuel cost, minimum wind and light abandon cost and maximum unit flexibility, the objective function is presented in Equation (19).

$$\min f_{\text{total}} = \sum_{t=1}^{T}\sum_{i=1}^{N_G}\left(a_i \cdot P_{i,t}^2 + b_i \cdot P_{i,t} + c_i\right) + \sum_{t=1}^{T} c_{aban}^{re}\left(\Delta P_{wT_t}^{av} + \Delta P_{pV_t}^{av}\right) - \sum_{t=1}^{T} c_s\left(F_{s,t}^{up} + F_{s,t}^{down}\right), \tag{19}$$

where N_G is the number of units; T is the total scheduling period; a_i, b_i, and c_i represent the generation cost coefficients of unit i; $P_{i,t}$ is the power of unit i at moment t; c_{aban}^{re} is the cost per unit of wind and photovoltaic abandonment; c_s is the incentive coefficient of the unit to provide the unit of adjustable power with flexibility; $\Delta P_{WT,t}^{av}$ and $\Delta P_{PV,t}^{av}$ are the average amount of electricity abandoned by wind power and photovoltaic power, respectively; $F_{s,t}^{up}$ and $F_{s,t}^{dowm}$ indicate the upward and downward adjusted flexibility supply for all units at moment t, respectively.

The flexibility supply of a unit refers to the ability of the unit to respond to uncontrollable changes in the system renewable energy and load power, related to its operating state

and inherent parameters. The upward flexibility and downward flexibility of all units at moment t are defined as follows:

$$F_{s,t}^{up} = \sum_{i=1}^{N_G} \min\left\{R_{g,i}^{u}, P_{g,i}^{\max} - P_{i,t}\right\}, \tag{20}$$

$$F_{s,t}^{down} = \sum_{i=1}^{N_G} \min\left\{R_{g,i}^{d} P_{i,t} - P_{g,i}^{\min}\right\}, \tag{21}$$

where $R_{s,i}^{u}$ and $R_{s,i}^{d}$ are the upper climbing rate and lower climbing rate of unit i, respectively; $P_{g,i}^{\max}$ and $P_{g,i}^{\min}$ indicate the upper and lower limits of the output of unit i, accordingly.

2. Restrictive condition

(1) Unit output constraint

$$u_{i,t} P_{g,i}^{\min} \le P_{i,t} \le u_{i,t} P_{g,i}^{\max}, \tag{22}$$

where $u_{i,t}$ denotes the state of unit i at moment t.

(2) Unit climbing constraints

$$P_{i,t} - P_{i,t-1} \le R_{g,i}^{u} u_{i,t-1} + S_i^{U}(u_{i,t} - u_{i,t-1}) + P_{g,i}^{\max}(1 - u_{i,t}), \tag{23}$$

$$P_{i,t-1} - P_{i,t} \le R_{g,i}^{d} u_{i,t} + S_i^{D}(u_{i,t-1} - u_{i,t}) + P_{g,i}^{\max}(1 - u_{i,t-1}), \tag{24}$$

where S_i^{U} and S_i^{D} are the start-up ramp-up and shutdown ramp-down limits for unit i, respectively.

(3) Flexibility supply constraints

$$\begin{cases} F_{i,t}^{up} \le R_{g,i}^{u} \cdot u_{i,t} \\ F_{i,t}^{up} \le \left(P_{g,i}^{\max} - P_{i,t}\right) \cdot u_{i,t} \\ F_{i,t}^{up} \ge 0 \end{cases}, \tag{25}$$

$$\begin{cases} F_{i,t}^{\text{down}} \le R_{g,i}^{d} \cdot u_{i,t} \\ F_{i,t}^{\text{down}} \le \left(P_{i,t} - P_{g,i}^{\min}\right) \cdot u_{i,t} \\ F_{i,t}^{\text{down}} \ge 0 \end{cases}, \tag{26}$$

where $F_{i,t}^{up}$ and $F_{i,t}^{\text{down}}$ are the upward flexibility supply and downward flexibility supply of unit i at moment t, respectively.

(4) Abandon wind and light constraints

The actual output of the wind power and photovoltaic power can be viewed as the predicted value superimposed on the random variable of the prediction error, i.e.,

$$P_t{}^{WT} = P_{f,t}^{WT} + \varepsilon_t{}^{WT}, \tag{27}$$

$$P_t^{PV} = P_{f,t}^{PV} + \varepsilon_t^{PV}, \tag{28}$$

where P_t^{WT} and P_t^{PV} are the actual output of the wind power and photovoltaic power at the moment t, respectively; $P_{f,t}^{WT}$ and $P_{f,t}^{PV}$ are the day-ahead predicted output of the wind power and photovoltaic power at the moment t, respectively; and ε_t^{WT} and ε_t^{PV} are the prediction errors of the wind power and photovoltaic power at the moment t, respectively. All of them are random variables.

The wind output value after wind and light abandonment should be between 0 and the installed capacity. The construction opportunity constraints are as follows:

$$P_r\left\{0 \le \left(P_{f,t}^{WT} - \Delta P_t^{WT}\right) + \varepsilon_t^{WT} \le S_{WT}\right\} \ge \delta_{WT}, \tag{29}$$

$$P_r\left\{0 \le \left(P_{f,t}^{PV} - \Delta P_t^{PV}\right) + \varepsilon_t^{PV} \le S_{PV}\right\} \ge \delta_{PV}, \tag{30}$$

where ΔP_t^{WT} and ΔP_t^{PV} are the abandoned power of the wind power and PV at the moment t, respectively; S_{WT} and S_{PV} indicate the installed capacity of the wind power and PV, respectively; δ_{WT} and δ_{PV} are the confidence level of the wind power and PV opportunity constraints, respectively; and Pr}} denotes the probability of the event being established.

(5) Power balance constraint

$$\sum_{i=1}^{N_G} P_{i,t} + \tilde{P}_t^{WT}\left(\varepsilon_t^{WT}\right) + \tilde{P}_t^{PV}\left(\varepsilon_t^{PV}\right) = P_{L,t}\left(\varepsilon_t^{L}\right), \tag{31}$$

where $\tilde{P}_t^{WT}\left(\varepsilon_t^{WT}\right)$ and $\tilde{P}_t^{PV}\left(\varepsilon_t^{PV}\right)$ represent the value of the wind power and photovoltaic output at moment t after power abandonment, respectively, corrected by prediction errors ε_t^{WT} and ε_t^{PD}, which are essentially random variables; $P_{L,t}\left(\varepsilon_t^{L}\right)$ refers to the total system load at moment t superimposed on the prediction error ε_t^{L}.

(6) Line transmission constraints

The transmission power of each branch is characterized based on the power current transfer distribution factor, as shown in the following equation:

$$P_{l,t}(z_t) = \sum_{i\in\Omega_G} G_{l-i}P_{i,t} + \sum_{m=\Omega_{WT}} G_{l-m}\tilde{P}_t^{WT}\left(\varepsilon_t^{WT}\right) + \sum_{m\in\Omega_{PV}} G_{l-n}\tilde{P}_t^{WT}\left(\varepsilon_t^{WT}\right) + \sum_{k=1}^{N_B} G_{l-k}P_{kf}^{L}\left(\varepsilon_{k,t}^{L}\right), \tag{32}$$

where $P_{l,t}(z_t)$ represents the transmission power of branch l at time t under the comprehensive influence of random variable z_t, in which, z_t is the set including random variables ε_t^{WT}, ε_t^{PV} and ε_t^{L}; G_{l-i} represents the power transfer distribution factor of bus i to branch l; Ω_G, Ω_{WT} and Ω_{PV} are the set of bus numbers of the unit, wind farm and photovoltaic power station, respectively; and N_B denotes the number of buses.

The line transmission power opportunity constraint is expressed as follows:

$$P_r\left\{-P_{l,\max} \le P_{l,t}(z) \le P_{l,\max}\right\} \ge \delta_l, \tag{33}$$

where $P_{l,\max}$ is the upper limit of the power transmission for branch l; δ_l is the confidence level of the chance constraint.

4.2.3. Model Transformation

The generalized polynomial chaos method is used to characterize the random variables ${\varepsilon_t}^{WT}$, ε_t^{PV}, and ε_t^{L}, to obtain the gPC basis function $\Phi_k(z_t)$. Then, the random variables in the system can be indicated by using the polynomial expansion as follows:

$$\begin{cases} \tilde{P}_{i,t}^{WT}\left(\varepsilon_t^{WT}\right) = \sum_{k=0}^{N_{gpc}} f_{i,k,t}^{WT}\Phi_k(z_t) \\ \tilde{P}_{j,t}^{PV}\left(\varepsilon_t^{PV}\right) = \sum_{k=0}^{N_{gpv}} f_{j,k,t}^{PV}\Phi_k(z_t) \\ P_{l,t}(z_t) = \sum_{k=0}^{N_{gpc}} f_{l,k,t}^{line}\Phi_k(z_t) \\ P_{n,t}^{L}\left(\varepsilon_{n,t}^{L}\right) = \sum_{k=0}^{N_{gpc}} f_{n,k,t}^{L}\Phi_k(z_t) \end{cases}, \tag{34}$$

where $P_{n,t}^{L}\left(\varepsilon_{n,t}^{L}\right)$ is the random variable of t bus n load at time t; $f_{i,k,t}^{WT}$, $f_{j,k,t}^{PV}$, $f_{l,k,t}^{line}$, and $f_{n,k,t}^{L}$ are the approximation coefficients of the wind power, photovoltaic power, line transmission power and bus load under the base function N_{gpc}, where the approximation coefficient of the line transmission power is the variable to be found; N_{gpc} is the order of gPC.

By further applying the Galerkin projection technology, and combining with the opportunity constraint conversion method based on the first and second moments, the lower model with the chance constraint can be transformed into a deterministic model:

1. Equation constrain transformation

The following equation is considered:

$$g(x, p(Z)) = 0, \tag{35}$$

where x is the variable to be sought, and $p(Z)$ is a random variable.

By the gPC characterization, the above formula can be rewritten as follows:

$$g\left(\sum_{k=0}^{N_{gpc}} x_k \Phi_k(z), \sum_{k=0}^{N_{gpc}} p_k \Phi_k(z)\right) = 0, \tag{36}$$

From Equation (13), if $f(Z) = 0$, the approximation coefficient of each term is also 0, and thus:

$$E\left(g\left(\sum_{k=0}^{N_{gpc}} x_k \Phi_k(Z), \sum_{k=0}^{N_{gpc}} p_k \Phi_k(Z)\right)\Phi_m(Z)\right) = 0, \tag{37}$$

Due to the expected operator, Equation (37) is a set of deterministic equations.

2. The inequality constraint transformation

The following inequality chance-constrained generic expressions are considered:

$$\Pr\{x \le a\} \ge \delta, \tag{38}$$

According to the distributional robust probability constraint lemma [28], the inequality chance constraint can be converted into convex second-order cone constraints on the generalized polynomial chaos coefficient, and combined Formulas (15) and (16), Formula (38) can be converted into the following form:

$$\kappa \cdot \sqrt{\sum_{k=0}^{N_{gpc}} \left(\gamma_k x_k^2\right)} + x_0 \le a, \tag{39}$$

where κ is the inequality constraint coefficient, and $\kappa = \sqrt{\delta/(1-\delta)}$.

4.3. Model Optimization

In this study, the flexibility supply capacity of two demand response resources, electric vehicles and air-conditioning clusters, is studied, and their adjustable potentials are evaluated using the Monte Carlo algorithm based on the method of research reported in [29]. Then, the probability distribution model of the adjustment capacity is established. By taking upward flexibility as an example, $F_{EV,t}^{up}(x)$ and $F_{AC,t}^{up}(x)$ are the upward flexibility supply probability distributions of electric vehicles and air-conditioning clusters at moment t, respectively. Then, the demand response upward flexibility $F_{DR,t}^{up}(x)$ can be expressed as follows:

$$F_{DR,t}^{up}(x) = F_{EV,t}^{up}(x) \oplus F_{AC,t}^{up}(x), \tag{40}$$

By overlaying the unit flexibility supply, the system upwardly adjusts the flexibility supply to the following:

$$F_{sys,t}^{up}(x) = F_{DR,t}^{up}\left(x + F_{s,t}^{up}\right), \tag{41}$$

Furthermore, based on Equation (6), the system upwardly adjusts the inflexibility expectation and adds a penalty term for cases where the inflexibility expectation is larger than a threshold. Considering the unit start-stop cost, wind and light abandonment cost, generation cost, and flexibility deficiency penalty, the system will keep searching for the

optimal solution with particle updating, and finally find the scheduling scheme with the lowest cost under the premise of satisfying the balance of the supply and demand of system flexibility.

5. Calculated Simulation

A case study is conducted using the IEEE-30 bus system, as shown in Figure 3, with the unit parameters detailed in Table A1 of Appendix A. Nodes 20 and 27 are connected to a wind farm and a photovoltaic power station, while nodes 16 and 19 are connected to clusters of electric vehicles and air conditioning systems. The day-ahead forecasts for wind and solar loads are illustrated in Figure 4. Based on the historical actual values and predicted values of the wind and solar output, along with the adjustable capacity assessment of the demand response resources, a second-order Gaussian mixture distribution is employed to probabilistically model the forecasting errors of the wind and solar output, as well as the flexibility supply from demand response, as detailed in Appendix A. It is assumed that the forecasting error for system load follows a normal distribution with a mean of 0 and a variance of 5% of the predicted value. The day-ahead scheduling period consists of 96 time slots over one day, and a second-order generalized polynomial chaos is used to construct basis functions to represent the random variables. The expected threshold for the system's flexibility supply-demand balance index is set at 0.05 p.u., with a reference power of 1000 MVA.

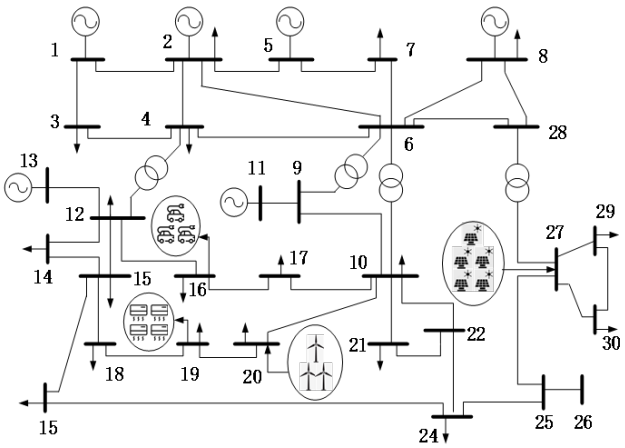


Figure 3. IEEE-30 system topology diagram.

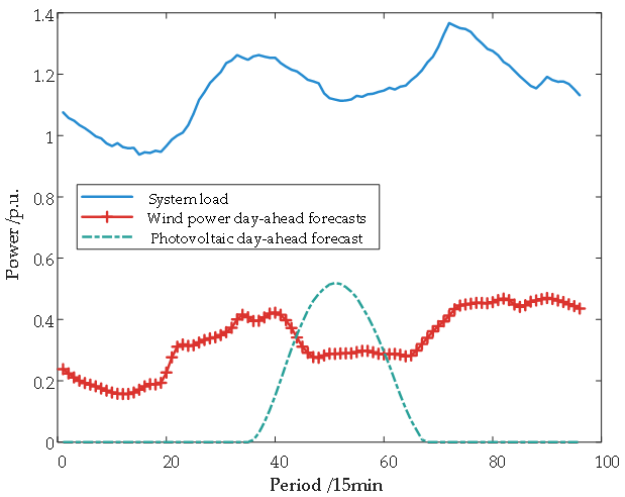


Figure 4. Day-ahead wind-photovoltaic-load forecasting values.

5.1. Optimal Scheduling Programme

Under the optimal dispatch scheme, the day-ahead output plan and the expected wind and PV output of each unit are shown in Figure 5, while the flexibility supply capacity provided by each unit at different times is displayed in Figure 6, and the unit start-up and shutdown scheme is presented in Figure 7. According to the figure, units 2 and 3 are enough to meet the load requirements of the system, while other units adjust the system flexibility by opening and shutting down.

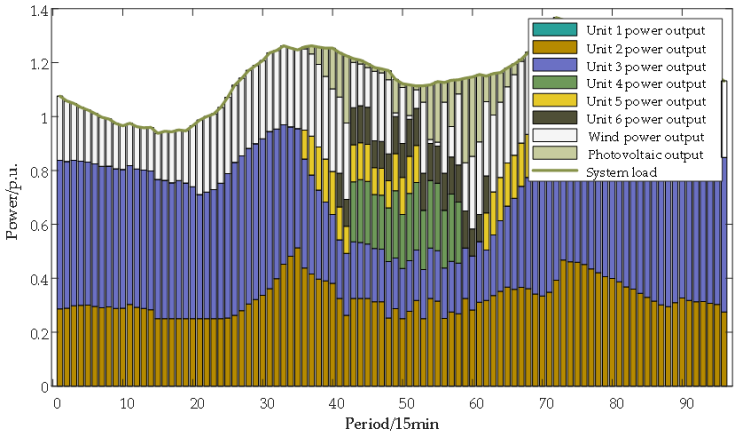


Figure 5. Day-ahead generation schedule.

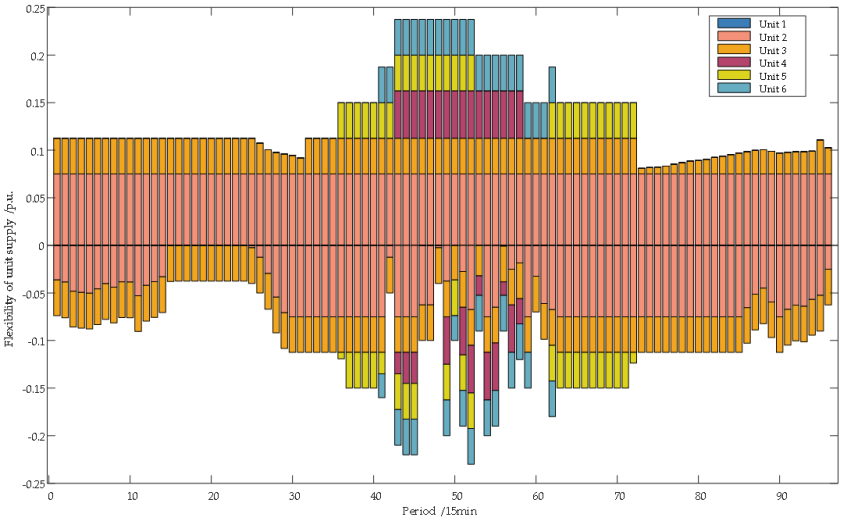


Figure 6. Flexibility supply of generator units.

Between moments 1 and 36, the PV output is 0 ; the system load is shared by the wind power, units 2# and 3#, and the system flexibility demand originates from the forecast error of the wind power and load. The net system load in this time period varies in the range of 0.68–0.88 p.u., which can be borne by unit 2# alone; however, this will result in unit 2# in a full-generation state, thus not being able to provide the flexibility supply capacity to address the uncontrolled stochastic fluctuations of the wind power and load. In this case, the situation of power and load abandonment will appear. At this time, the system flexibility demand is relatively low, through the reasonable distribution of the net load between unit 2# and 3#, not only to ensure that the system has sufficient flexibility supply, but also to avoid large economic costs. Similarly, between 67 and 96, units 3# and 4# take on the role of generating power and providing flexibility.

Between moments 37 and 66, the power fluctuation of PV leads to further enhancement of the system flexibility demand, and the strong uncertainty of the wind load prediction error at individual moments makes the system flexibility balance situation tense. At this

time, units 4#, 5#, and 6# provide additional flexibility supply by switching on the power to alleviate the pressure on the system balance.

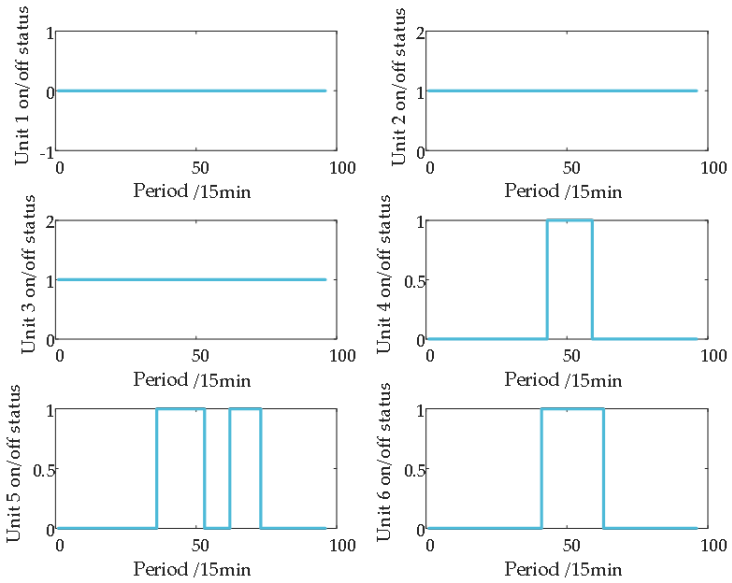


Figure 7. Flexibility supply of generator units.

The system flexibility supply and demand balance indexes for each time period are shown in Figure 8, which fully exploit the flexibility regulation potential of the source side through unit startup and shutdown and reasonable output allocation, and the system's flexibility deficit expectation for each time period is within the threshold. This improves the system's balancing capability under the active uncertainty of the source and load sides. Figure 9 presents the probability distribution of the upward flexibility balancing margin for the system considering only the demand response and jointly taking into account the demand response and the unit flexibility supply under moment 55. Apart from that, the corresponding upward flexibility insufficiency expectations of the two are 0.31 p.u. and 0.03 p.u., respectively, which shows that the adjustable potentials of the source and load sides need to be fully exploited in the high-ratio new energy system and that further consideration of the system flexibility balancing capability in the day-ahead dispatch scheme contributes to improving the system balancing capability under the active uncertainty of the source and load sides. In addition, involving the system flexibility balancing capability is conducive to enhancing the safety and stability of the system.

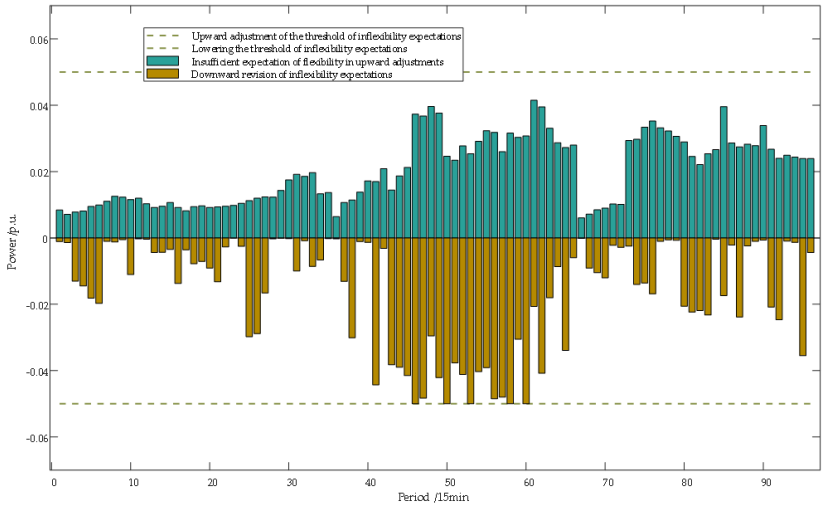


Figure 8. System flexibility supply-demand balance indicators.

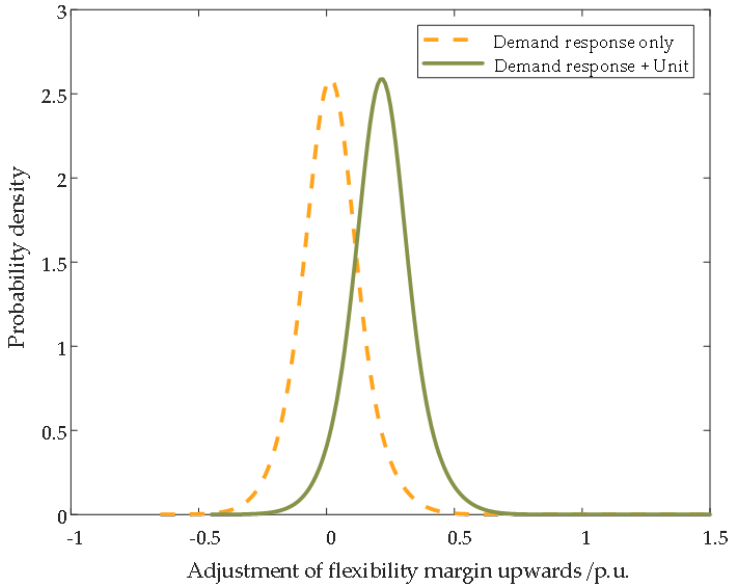


Figure 9. Probability distribution of flexibility margin for system upregulation.

5.2. Impact of Different Scheduling Options on System Flexibility

To further illustrate the effectiveness of the proposed model, the flexibility balance index and economy of the system under three different scheduling schemes are compared. Among them, Scenario 1 is the optimal scheduling scheme formulated by the model proposed in this paper; Scenario 2 is the conventional economic scheduling method, and Scenario 3 is the scheduling scheme generated by the model proposed in this paper during the iterative process. The downward flexibility deficit expectation of the system at the 37–66 moments under each scheme is displayed in Figure 10, and the comparison of operating costs is presented in Table 2.

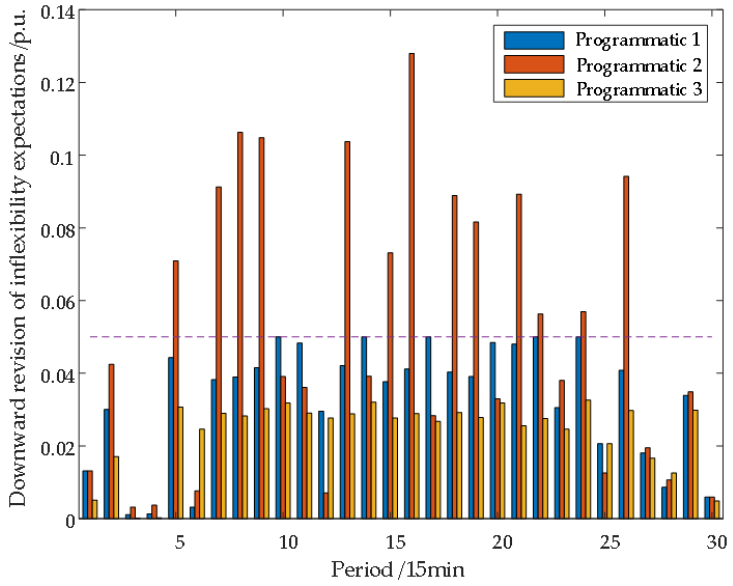


Figure 10. Expected value of insufficient flexibility in system down-regulation under different scheduling schemes.

As shown in Figure 10 and Table 2, Scenario 2 exhibits the lowest system operating costs; however, the flexibility supply under this option is significantly less than the demand, preventing the system from effectively addressing the random fluctuations in the source load. Scenario 3 satisfies the constraints of the system flexibility index and offers the highest

flexibility supply capacity, resulting in a near-zero risk of power abandonment and load shedding, although this scenario incurs a higher economic cost. Scenario 1 not only meets the system flexibility constraints but also achieves a considerably lower total economic cost. This indicates that the optimal scheduling scheme developed in this research ensures a balance between system flexibility and operational economy, thereby demonstrating the effectiveness of the proposed model.

Table 2. System operating costs under different scheduling schemes.

Programme	Start-Stop Cost (¥ Million)	Abandoned Electricity Costs (¥ Million)	Power Generation Costs (¥ Million)	Total Cost (¥ Million)
1	14.75	0.1254	2753.92	2768.80
2	14.00	0.0831	2052.34	2066.42
3	11.50	0.1577	3062.63	3074.29

5.3. Validation of gPC Validity

To verify that the generalized polynomial chaos (gPC)-based approximation principle effectively characterizes the uncertainty of tidal currents influenced by multidimensional random variables, Figure 11 compares the probability density function of the transmission power of branch 55 at a specific moment, as obtained by the second-order gPC method and the Monte Carlo simulation method. The root-mean-square error of the gPC fitting is 0.00032, indicating that the second-order method can characterize the uncertainty of tidal currents with high accuracy. Consequently, the uncertainty of the tidal currents is maintained within a certain confidence level, ensuring that the line transmission power remains within acceptable limits and reducing the risk of network blocking.

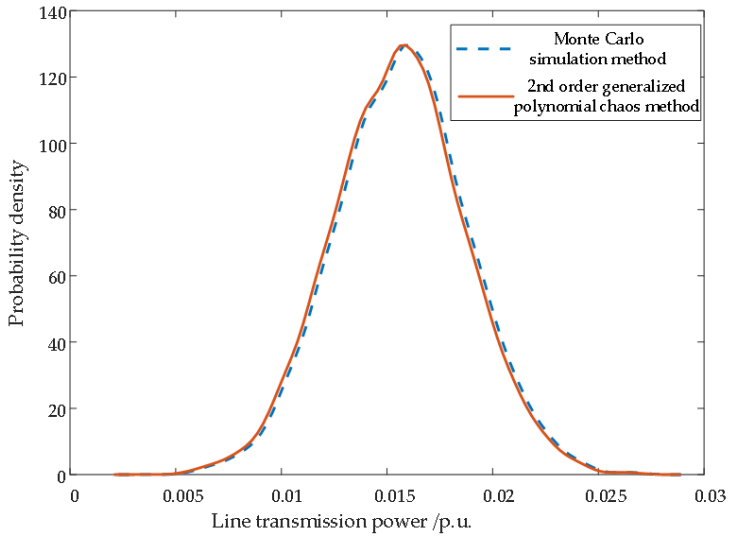


Figure 11. Probability density function of transmission power on branch 5 at time 55.

6. Summary

The integration of a high proportion of renewable energy sources has resulted in increasingly stringent flexibility requirements for power systems. Therefore, it is essential to construct a probabilistic assessment framework for flexibility and formulate corresponding scheduling strategies. This study proposes a two-tier scheduling model for the day-ahead scheduling of renewable energy systems with a high proportion of renewables, considering both flexibility balancing capabilities and economic factors. The main conclusions are as follows:

(1) System flexibility evaluation: This research defines a flexible power balance index and constructs an opportunity constraint model. The model evaluates system flexibility from the perspectives of supply and demand balance and transmission. It aims to prevent power failures and load rejection caused by insufficient adjustable capacity or line blockage.

(2) Flexibility and economy balance: The model enhances the system's balancing ability at a lower cost through the start and stop operations of units. In particular, under conditions of uncertainty regarding active power on both the supply and load sides, the model demonstrates effective balancing capabilities.

(3) Application of the gPC method: The generalized Polynomial Chaos (gPC) method effectively characterizes the current uncertainties influenced by multidimensional random variables with different distribution characteristics. This method reduces the risk of network blockage and ensures the safe and stable operation of the power grid.

Author Contributions: Conceptualization, W.X.; data curation, W.X., P.W. and S.L.; formal analysis, Z.Y.; methodology, Z.Y., P.W. and N.S.; software, P.W.; validation, N.S. and S.L.; writing—original draft, Z.Y.; writing—review and editing, W.X., P.W., N.S. and S.L. All authors have read and agreed to the published version of the manuscript.

Funding: This research received no external funding.

Data Availability Statement: The original contributions presented in the study are included in the article, further inquiries can be directed to the corresponding author.

Acknowledgments: This work was supported by the scientific and technological project of the Central China Division of Power Grid, "Research on the key technology of cross-provincial peak-peak supply protection adapted to the constraints of multiple cross-sections" (Project No.:521400230001).

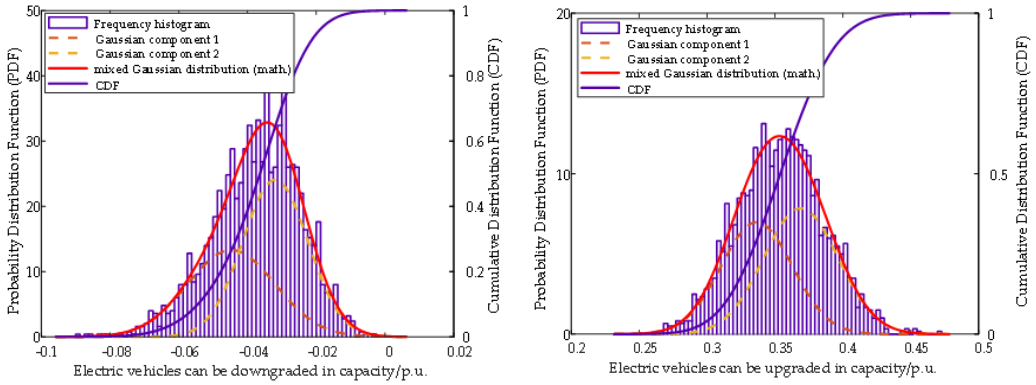
Conflicts of Interest: Authors Zheng Yang and Wei Xiong were employed by the Central China Branch of State Grid Corporation of China. The remaining authors declare that the research was conducted in the absence of any commercial or financial relationships that could be construed as a potential conflict of interest.

Appendix A

Table A1. The parameters of power generating units.

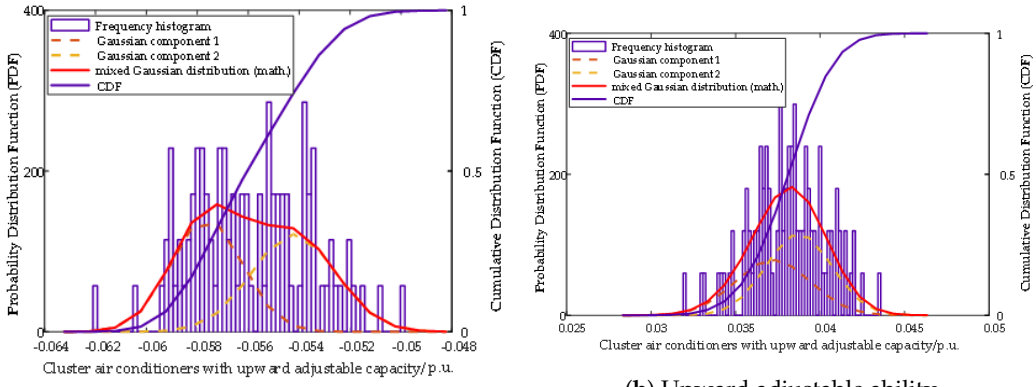
Unit Number	Access Node	$P_{g,i}^{max}$ (p.u.)	$P_{g,i}^{min}$ (p.u.)	a_i (yuan /(p.u.)^2)	b_i (yuan/p.u.)	c_i (yuan)	$R_{g,i}^{u}/R_{g,i}^{d}$ (p.u./h)	$T_{O,i}/T_{S,i}$ (h)	Start-Up Cost (yuan/event)	Shutdown Costs (yuan/event)
1#	1	1.5749	0.5	0.1524	38.5397	786.7988	0.375	2	39,372.5	19,686.25
2#	2	1	0.25	0.1058	46.1591	945.6332	0.3	2	25,000	12,500
3#	5	0.6	0.15	0.028	40.3965	1049.998	0.15	2	15,000	7500
4#	8	0.8	0.2	0.0354	38.3055	1243.531	0.2	2	20,000	10,000
5#	11	0.4	0.1	0.0211	36.3278	1658.57	0.15	2	10,000	5000
6#	13	0.4	0.1	0.0179	38.2704	1356.659	0.15	2	10,000	5000

Taking moment 50 as an example, the Monte Carlo method is used to simulate the electricity consumption behavior of EV clusters and air-conditioning loads, and assess their up-regulatable and down-regulatable capacities. And the second-order Gaussian mixture distribution is used to construct the adjustable capacity probability model, which is shown in Figures A1 and A2. In addition, the historical power data of a wind farm and a photovoltaic power plant in central China are utilized to build the corresponding forecast error probability distribution models, respectively, as shown in Figures A3 and A4.



(**a**) Downward adjustable ability; (**b**) Upward adjustable ability.

Figure A1. Probability distribution of adjustable capacity of electric vehicles.



(**a**) Downward adjustable ability; (**b**) Upward adjustable ability.

Figure A2. Probability distribution of adjustable capacity of air conditionings.

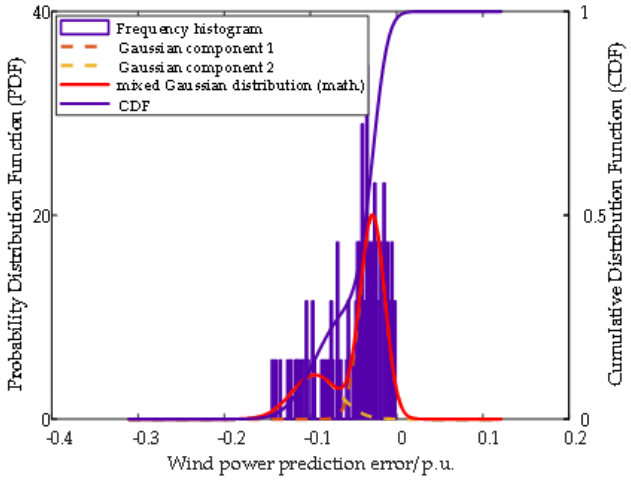


Figure A3. Probability distribution of wind power prediction error.

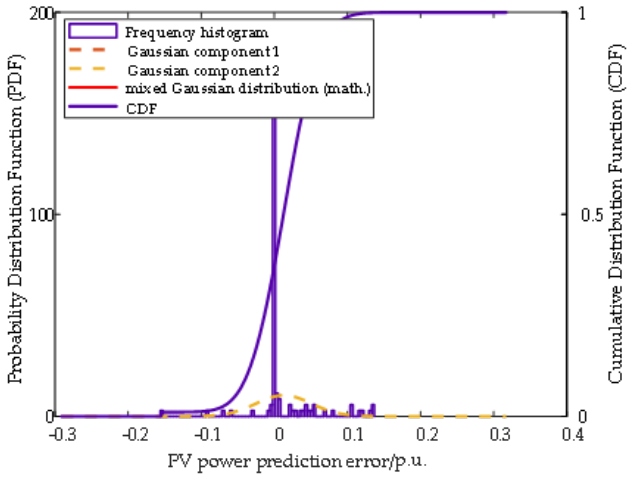


Figure A4. Probability distribution of photovoltaic power prediction error.

References

1. Ju, L.; Lv, S.; Li, P. Research review of novel demand-Side flexibility resource spatio-temporal co-optimization and dynamic equilibrium mechanism of power systems. *Electr. Power Constr.* **2024**, *45*, 142–163.
2. Lu, Z.; Li, H.; Qiao, Y. Flexibility evaluation and supply/demand balance principle of power system with high-penetration renewable electricity. *Proc. CSEE* **2017**, *37*, 9–20.
3. Zhang, H.; Chen, W.; Shen, J. Review of power distribution network resilience considering flexibility resources. *Electr. Power Constr.* **2023**, *44*, 66–84.
4. Jin, C.; Ren, D.; Xiao, J.; Hou, J.; Du, E.; Zhou, Y. Optimization planning on power system supply-grid-storage flexibility resource for supporting the "carbon neutrality" target of China. *Electr. Power* **2021**, *54*, 164–174.
5. Wang, Q.; Wang, L.; Gui, Q. Power system unit commitment with large-scale wind power considering multi-time scale output flexibility. *Smart Power* **2021**, *49*, 35–41, 70.
6. Bagherinezhad, A.; Khatami, R.; Parvania, M. Continuous-time look-ahead flexible ramp scheduling in real-time operation. *Int. J. Electr. Power Energy Syst.* **2020**, *119*, 105895. [CrossRef]
7. Zhengyi, L.; Jinqing, P.; Rongxin, Y. Many-objective day-ahead optimal scheduling of residential flexible loads integrated with stochastic occupant behavior models. *Appl. Energy* **2023**, *347*.
8. Wu, H.; Shahidehpour, M.; Li, Z.; Tian, W. Chance-Constrained Day-Ahead Scheduling in Stochastic Power System Operation. *IEEE Trans. Power Syst.* **2014**, *29*, 1583–1591. [CrossRef]
9. Li, Y.; Hu, B.; Xie, K.; Wang, L.; Xiang, Y.; Xiao, R.; Kong, D. Day-Ahead Scheduling of Power System Incorporating Network Topology Optimization and Dynamic Thermal Rating. *IEEE Access* **2019**, *7*, 35287–35301. [CrossRef]
10. Sun, Y.; Zhang, B.; Ge, L.; Sidorov, D.; Wang, J.; Xu, Z. Day-ahead optimization schedule for gas-electric integrated energy system based on second-order cone programming. *CSEE J. Power Energy Syst.* **2020**, *6*, 142–151.
11. Sun, G.; Yuan, Z.; Geng, T.; Wang, Y.; Wei, Z.; Zang, H. Robust stochastic optimal dispatching of virtual power plant containing plug-in electric vehicles. *Autom. Electr. Power Syst.* **2017**, *41*, 44–50+79.
12. Lv, X.; Liu, T.; Liu, X.; He, C.; Nan, L.; Zeng, H. Low-carbon economic dispatch of multi-energy park considering high proportion of renewable energy. *J. Shanghai Jiaotong Univ.* **2021**, *55*, 1586–1597.
13. Gan, L.; Chen, X.; Yu, K.; Zheng, J.; Du, W. A probabilistic evaluation method of household EVs dispatching potential considering users' multiple travel needs. *IEEE Trans. Ind. Appl.* **2020**, *56*, 5858–5867. [CrossRef]
14. Yan, H.; Hu, J.; Huang, D.; Zhang, Z.; Yue, Y. Distribution network planning considering the flexibility of EV virtual power plants and high penetration of PV. *Electr. Power Constr.* **2022**, *43*, 14–23.
15. Han, L.; Chen, S.; Wang, S. Scheduling strategy considering wind and photovoltaic power consumption and the flexibility of electric vehicles. *Trans. China Electrotech. Soc.* **2024**, 1–11.
16. Niu, H.; Li, Y.; Zhang, Q. Research on integrated energy day-ahead scheduling method taking into account source-side uncertainty. *Process Autom. Instrum.* **2024**, *45*, 41–47.
17. Chen, K.; Chen, W.; Lin, C.; Zhang, S.; Yu, D.; Yang, Y.; Chen, Z.; Lai, L. Integrated energy system day-ahead dispatch considering supply-side and demand-side flexibility. In Proceedings of the 2021 IEEE 5th Conference on Energy Internet and Energy System Integration (EI2), Taiyuan, China, 22–24 October 2021; pp. 1662–1667.
18. Bian, X.; Sun, M.; Dong, L.; Yang, X.W. Distributed source-load coordinated dispatching considering flexible aggregated power. *Autom. Electr. Power Syst.* **2021**, *45*, 89–98.
19. Chen, P.; Zhen, Z.; Wang, F. Day-ahead Modified Dispatching Model Considering Power System Flexibility. In Proceedings of the 2021 IEEE Industry Applications Society Annual Meeting (IAS), Vancouver, BC, Canada, 10–14 October 2021; pp. 1–6.

20. Tao, Y.; Wang, Q.; Yin, Z.; Zhang, H.; Liao, K. A Flexibility-Based Two-Stage Optimization Method for Day-Ahead and Intra-Day Scheduling of Coal-Hydro-Wind-Photovoltaic Multi-Energy Power System. In Proceedings of the 2023 2nd Asian Conference on Frontiers of Power and Energy (ACFPE), Chengdu, China, 20–22 October 2023; pp. 666–672.
21. Huang, X.; Feng, Y. Day-ahead and intra-day coordinated optimal scheduling of stand-alone microgrid considering unit flexibility. *Electr. Power Autom. Equip.* **2020**, *40*, 125–131.
22. Xiao, B.; Yu, L.; Liu, H.B.; Yan, G.G.; Dong, L.; CH, M. Day ahead optimal dispatch of multi-energy power system based on generating virtual net load. *Proc. CSEE* **2021**, *41*, 7237–7249.
23. Xiao, B.; Zhang, B. Day-ahead optimal scheduling of multi-energy power systems considering power source flexibility and complementarity. *Hunan Electr. Power* **2023**, *43*, 16–23.
24. Zhang, G.; Li, F. Day-ahead optimal scheduling of power system considering comprehensive flexibility of source-load-storage. *Power Autom. Equip.* **2020**, *40*, 159–167.
25. Lu, Z.; Li, H.; Qiao, Y. Power system flexibility planning and challenges considering high proportion of renewable energy. *Autom. Electr. Power Syst.* **2016**, *40*, 147–158.
26. Jiang, T.; Li, C.; Zhang, R. Probabilistic available transfer capacity evaluation of power systems using polynomial chaos expansion. *Proc. CSEE* **2024**, *44*, 489–504.
27. Huang, M.; Wang, P.; Zhang, Q. Comprehensive Evaluation of Demand Response Resource Participation in Grid FM Taking into Account Regulation Performance and Economy. *J. Wuhan Univ. (Eng. Ed.)* **2022**, *55*, 822–832. [CrossRef]
28. Calafiore, G.C.; Ghaoui, L.E. On distributionally robust chance-constrained linear programs. *J. Optim. Theory Appl.* **2006**, *130*, 1–22. [CrossRef]
29. Wang, C. Research on Aggregated Operational Characteristics and Uncertainties of Demand Side Resources. Ph.D. Thesis, Beijing Jiaotong University, Beijing, China, 2021.

Disclaimer/Publisher's Note: The statements, opinions and data contained in all publications are solely those of the individual author(s) and contributor(s) and not of MDPI and/or the editor(s). MDPI and/or the editor(s) disclaim responsibility for any injury to people or property resulting from any ideas, methods, instructions or products referred to in the content.